

Article

Study on Sulfuric Acid Leaching and Purification of Zinc Ferrite by Roasting Zinc-Containing Gossan Ore

Jinlin Yang¹, Hangyu Li¹, Zongyu Li¹, Xingnan Huo¹, Shizhen Liao¹, Shaojian Ma¹ and Hengjun Li^{2,*}

¹ State Key Laboratory of Featured Metal Materials and Life-Cycle Safety for Composite Structures, MOE Key Laboratory of New Processing Technology for Nonferrous Metals, Guangxi Higher School Key Laboratory of Minerals Engineering and Materials, College of Resources, Environment and Materials, Guangxi University, Nanning 530004, China

² College of Chemistry and Chemical Engineering, Guangxi University, Nanning 530004, China

* Correspondence: 1615302001@st.gxu.edu.cn; Tel.: +86-131-5266-0958

Abstract: Gossan discarded from mining processes result in metal resource wastage, and its long-term stacking causes environmental hazards. Therefore, this article considers zinc-containing gossan as the research object. The ore was roasted to prepare primary zinc ferrite products and sulfuric acid leaching was performed for purification. Then, XRD analysis was performed to characterize the purified products. The results indicated that the effect of sulfuric acid concentration on the purification of the products was related to its zinc ferrite content. Furthermore, the effect of leaching temperature on the purification of zinc ferrite products was related to sulfuric acid concentration; the lower the sulfuric acid concentration, the more considerable the effect of leaching temperature. The conditions suitable for purifying the products through sulfuric acid leaching are as follows: sulfuric acid concentration of 140 g/L, liquid–solid ratio of 4:1, leaching temperature of 80 °C, leaching time of 120 min, and stirring speed of 300 rpm. This article determines the factors affecting the purification of zinc ferrite by sulfuric acid leaching along with the optimal purification conditions. The findings presented herein provide a theoretical foundation for the development of new processes for preparing zinc ferrite, which has considerable industrial application value.

Keywords: gossan ore; zinc ferrite; leaching; purification



Citation: Yang, J.; Li, H.; Li, Z.; Huo, X.; Liao, S.; Ma, S.; Li, H. Study on Sulfuric Acid Leaching and Purification of Zinc Ferrite by Roasting Zinc-Containing Gossan Ore. *Processes* **2023**, *11*, 2149. <https://doi.org/10.3390/pr11072149>

Academic Editor: Carlos Sierra Fernández

Received: 15 June 2023
Revised: 13 July 2023
Accepted: 17 July 2023
Published: 19 July 2023



Copyright: © 2023 by the authors. Licensee MDPI, Basel, Switzerland. This article is an open access article distributed under the terms and conditions of the Creative Commons Attribution (CC BY) license (<https://creativecommons.org/licenses/by/4.0/>).

1. Introduction

Gossan ore has a low precious metal content and high development costs and has generally been neglected. With the extensive development and utilization of mineral resources, the ore grade has gradually depleted and mineral resources are gradually becoming more complex. High-grade, easy-to-mine, easy-to-grind, and easy-to-select mineral resources have increasingly depleted and now there remains low-grade and complex mineral raw materials [1]. Generally, gossan ore is a waste rock in the process of sulfide mining. This is because gossan ore is located in the upper part of sulfide deposits, and it is necessary to remove gossan ore to create suitable conditions for mining sulfide ore in lower parts. However, the discarded gossan ore not only causes waste of metal resources but also poses an environmental pollution risk due to long-term stacking. Different types of primary sulfide deposits form gossans through surface oxidation, and their elemental combinations differ [2]. Although there are many precious metals in gossan ore, effective recovery and utilization of its resources is difficult due to its oxidized nature and low metal content. Therefore, researchers have conducted few studies and only determine the type and content of mineral deposits, as well as the effects of heavy metal components in gossan ore on the environment [3–9]. For example, Juan studied the biological oxidation of black gossan and developed new methods for recovering lead, silver, and gold [10]. Mohamed studied the adsorption performance and adsorption mechanism of Cr (VI) on porous nanocomposites prepared at the interface of gossan ore and modified coal [11]. Dunn investigated the

reactivation of gold in gossans [12]. Santoro conducted a comprehensive evaluation of the trace element footprint of FeO/OH in residual zones (gossan) at the top of the oxidized ore body to determine parameters controlling the enrichment process of metals in ores [13]. In summary, research on gossan ore resources has primarily focused on the recovery of precious metals, while neglecting other aspects.

Preliminary research has found that zinc-containing gossan ore contains simple minerals, such as limonite, smithsonite, hemimorphite, and quartz; however, the mineral relationship is particularly complex [14]. This indicates that although the ore is oxidized, its elemental occurrence state is different from most oxidized ores. Therefore, the utilization of this ore requires the development of new beneficiation and smelting technologies. Studying zinc-containing gossan ore as a specialized research object and employing new processing technologies has considerable academic value. Notably, the ore contains high levels of zinc and iron minerals, and substances such as zinc ferrite were obtained during roasting [15].

Zinc ferrite is not easily decomposed at high temperatures, and is insoluble in weak acids and alkalis. Owing to these characteristics, zinc ferrite can be utilized to prepare high-temperature and corrosion-resistant nontoxic coatings [16]. Zinc ferrite exhibits soft magnetism and can be used to prepare magnetic devices, such as electromagnetic switches [17–19]. In addition, it has excellent photocatalytic performance and can be used to prepare catalysts for the degradation of water pollutants [20–22]. Further, it possesses optimal absorbing properties and, thus, can be used in composite materials to improve dielectric loss, enhance material resistance to electromagnetic wave radiation, and enhance the absorption properties of coating materials [23]. However, there are very few natural zinc ferrite minerals in nature, and the artificial synthesis of zinc ferrite suffers from issues such as high raw material costs, complex production processes, low yield, and high prices.

For gossan ore with abundant resources and high utilization potential, a lack of targeted basic research and efficient new technologies will be extremely unfavorable for the rational development and utilization of this mineral resource in the future, resulting in resource waste and adverse economic and environmental consequences. Therefore, this article considers gossan ore as the research object. Based on a new approach to mineral processing technology, the study employs a roasting method to prepare zinc ferrite, followed by a sulfuric acid leaching method to purify the prepared zinc ferrite. XRD analysis is performed to characterize purified zinc ferrite, with a focus on investigating the effect of sulfuric acid concentration, liquid–solid ratio, and other factors on purification. Investigating the effect of factors such as stirring speed in leaching on the purification of zinc ferrite provides a theoretical foundation for the development of new processes for preparing zinc ferrite with considerable value in industrial applications.

2. Materials and Methods

2.1. Materials

The raw materials used in this experiment were zinc-containing gossan ore collected from a certain mine. Before the experiment, the samples were crushed to the particle size of -0.074 mm. The crushing equipment was a jaw crusher, and the screening equipment was a vibrating screen. ZnO and Fe₂O₃ were used to adjust the molar ratio of zinc to iron.

The multi-element semiquantitative analysis results are shown in Table 1. The equipment was an X-ray fluorescence element analyzer.

Table 1. The multi-element semiquantitative analysis results of gossan ore (source: [15,24]).

Component	Zn	Fe ₂ O ₃	SiO ₂	Al ₂ O ₃	MgO	CaO
Content (%)	8.99	68.32	10.32	5.6	1.35	0.56
Component	Na ₂ O	K ₂ O	SO ₃	TiO ₂	Mn	Pb
Content (%)	0.20	0.12	0.90	0.25	1.46	1.38

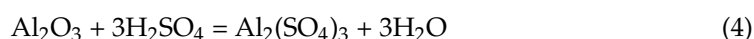
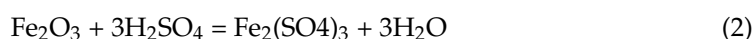
From Table 1, it can be seen that the element composition of the gossan ore was mainly composed of zinc, iron, and silicon. The content of iron in this sample is 47.82% and the content of zinc is 8.99%.

2.2. Experimental Principles and Characterization Methods

2.2.1. Test Methods and Principles

In the experimental method, -0.074 -mm particles of gossan ore are roasted to prepare zinc ferrite having impurities, followed by leaching with sulfuric acid for purification. Finally, the content of zinc ferrite in the obtained leaching residue is determined. The roasting is divided into two groups: high- and low-temperature roasting. The experimental conditions are as follows: (1) By adding ZnO or Fe₂O₃, the Zn/Fe molar ratio of the reactant is adjusted to 1:2. Further, the mechanical activation time is 120 min, the roasting temperature is 1050 °C, and the roasting time is 120 min. A zinc ferrite content of 88.6% was obtained under these preparation conditions (high-content zinc ferrite, Sample A). (2) By adding zinc or iron oxide, the Zn/Fe molar ratio of the reactant is adjusted to 1:2. Further, the mechanical activation time is 120 min, the roasting temperature is 800 °C, and the roasting time is 120 min. Accordingly, a zinc ferrite content of 75.3% was obtained as the product (low-content zinc ferrite, Sample B). Finally, purification through sulfuric acid leaching was conducted on Samples A and B to investigate the effects of sulfuric acid concentration, temperature, liquid–solid ratio, time, and stirring speed on the purification.

The main chemical reactions that may occur in the experiment are as follows:



2.2.2. Characterization Methods

XRD analysis is the primary method employed in experiments for characterization. The quantitative analysis of zinc ferrite is mainly performed using Jade software. Due to the presence of various impurities in mineral samples, as well as the possibility of unreacted zinc and iron oxide minerals, generally, quantitative methods cannot determine the specific content of zinc ferrite. In XRD analysis, the diffraction intensity of different substances in the mixture increases with the relative content of the substances in the mixture. Therefore, the intensity of the ferrite zinc diffraction peak in XRD analysis can be used to calculate its content.

3. Results

3.1. Effect of Sulfuric Acid Concentration

Sulfuric acid leaching for purification was conducted on Samples A and B to investigate the effect of sulfuric acid concentration on the purification of zinc ferrite. The leaching test conditions are as follows: 50 g of Samples A and B is used; the liquid–solid ratio is 7:1; the leaching temperature is 80 °C; the leaching time is 120 min; the stirring speed is 300 rpm; and the sulfuric acid concentrations are 20, 40, 60, 80, 100, 120, 140, 160, 180, 200, 220, 240, 260, 280, and 300 g/L. The effect of sulfuric acid concentration on zinc ferrite content in the leaching residue of Samples A and B is depicted in Figure 1. The XRD patterns of the leaching residue of Samples A and B under different sulfuric acid concentrations are shown in Figure 2.

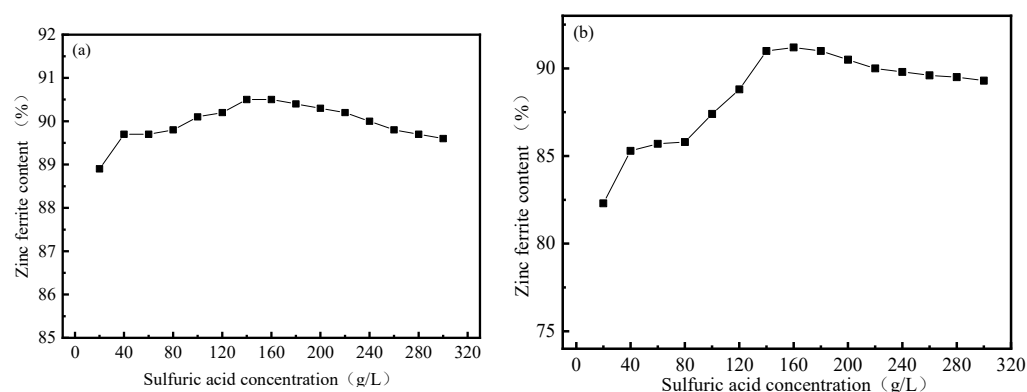


Figure 1. Effect of sulfuric acid concentration on the content of zinc ferrite in leaching residue: (a) Sample A; (b) Sample B.

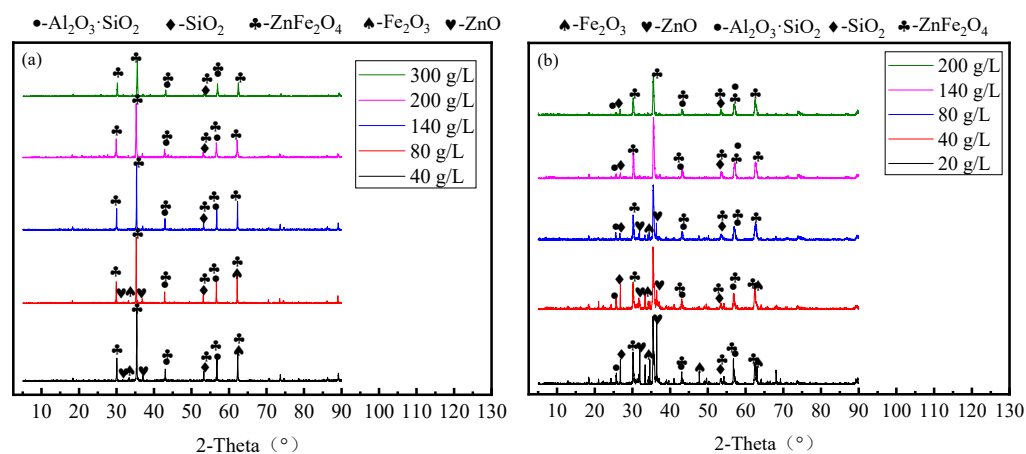


Figure 2. XRD patterns of leaching residues of zinc ferrite product under different sulfuric acid concentrations: (a) Sample A; (b) Sample B.

As shown in Figure 1, the patterns of Samples A and B are similar. When the concentration of sulfuric acid is <40 g/L, zinc ferrite content in the leaching product of Samples A and B increases rapidly, indicating that soluble impurities have been dissolved. When the concentration of sulfuric acid is 40–80 g/L, the increase in zinc ferrite content in Samples A and B is insignificant. This may be due to insufficient acidity, which prevents insoluble impurities in the roasted product from being dissolved. At a sulfuric acid concentration of 80–140 g/L, zinc ferrite content in Samples A and B continues to increase gradually, which may be due to the solution acidity being able to dissolve insoluble impurities in the roasted product. When sulfuric acid concentrations exceed 140 g/L, zinc ferrite in Samples A and B is gradually dissolved, decreasing its content in the leached products.

As shown in Figure 2a, when the amount of sulfuric acid used is relatively low (40 and 80 g/L), even Sample A with a high-zinc ferrite content has a small amount of Fe₂O₃ and ZnO that cannot be dissolved after leaching. Specifically, the diffraction peaks of Fe₂O₃ and ZnO can be seen in the XRD spectra of 40 g/L and 80 g/L leaching residues. Through XRD quantitative analysis, the zinc ferrite content in the leaching residues is found to be 89% and 89.5% for Sample A and Sample B, respectively. When the sulfuric acid concentration reaches 140 g/L, the diffraction peaks of Fe₂O₃ and ZnO in the XRD spectrum of the leaching residues disappear, and the zinc ferrite content in the leaching residues reaches 90.7%. When the sulfuric acid concentration reaches 200 and 300 g/L, the diffraction peak intensity of zinc ferrite decreases, indicating that at this sulfuric acid concentration, zinc ferrite in the samples begins to dissolve. At these concentrations, zinc ferrite content in the leaching residues is 89.8% and 88.8% for Sample A and Sample B, respectively. Therefore, for Sample A, having a high content of zinc ferrite indicates that

the purification effect of sulfuric acid leaching is insignificant. Figure 2b shows that after Sample B was leached with low-concentration sulfuric acid (20 g/L), impurities in the sample were not effectively removed; there were several diffraction peaks of Fe_2O_3 and ZnO in the XRD spectrum. Zinc ferrite content in the leaching residue of this sample was 77.8%. At a sulfuric acid concentration of 40 g/L, the diffraction peak intensities of Fe_2O_3 and ZnO in Sample B were significantly decreased; the zinc ferrite content in the leaching residue was 85.3%. At a sulfuric acid concentration of 140 g/L, the diffraction peak intensity of impurities in Sample B further decreased, and the zinc ferrite content in the leaching residue reached 91%. When the concentration of sulfuric acid further increased to 200 g/L, the diffraction peaks of Fe_2O_3 and ZnO were not clearly seen in the diffraction spectrum. Furthermore, as the sulfuric acid concentration increased, the diffraction peak intensity of zinc ferrite decreased, indicating that zinc ferrite in the leaching residue was partially dissolved. Therefore, the sulfuric acid leaching purification effect is more visible in the low-content zinc ferrite Sample B than in Sample A.

3.2. Effect of Leaching Temperature

According to the results presented in Section 3.1, the leaching and purification effect on Sample B having low-zinc ferrite content is better. Therefore, from the perspective of energy efficiency and simplification of the phase composition of reaction products, Sample B was selected for all subsequent sulfuric acid leaching and purification experiments.

The experimental conditions for sulfuric acid leaching are as follows: 50 g of Sample B is used; the sulfuric acid concentrations are 40, 80, and 140 g/L; the liquid–solid ratio is 7:1; the leaching temperatures are 25 °C, 35 °C, 45 °C, 55 °C, 65 °C, 75 °C, 80 °C, and 85 °C; leaching time is 120 min; and the stirring speed is 300 rpm. The effect of leaching temperature on the zinc ferrite content in the leaching residues at different sulfuric acid concentrations is depicted in Figure 3.

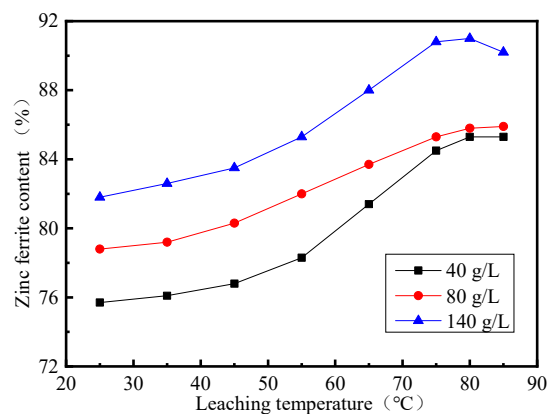


Figure 3. Effect of leaching temperature on zinc ferrite content for different sulfuric acid concentrations.

As shown in Figure 3, at a low sulfuric acid concentration (40 g/L), leaching temperature has a considerable effect on the purification of zinc ferrite. When the concentration of sulfuric acid is >140 g/L, leaching temperature has a slight effect on the purification of zinc ferrite. When the leaching temperature is 80 °C, zinc ferrite content in the product reaches 91%. As the temperature increase, the zinc ferrite content slightly decreases, probably because higher leaching temperatures promote the dissolution of zinc ferrite at high sulfuric acid concentrations.

The XRD spectra of leaching residues of Sample B at different leaching temperatures and sulfuric acid concentrations of 40, 80, and 140 g/L are shown in Figure 4.

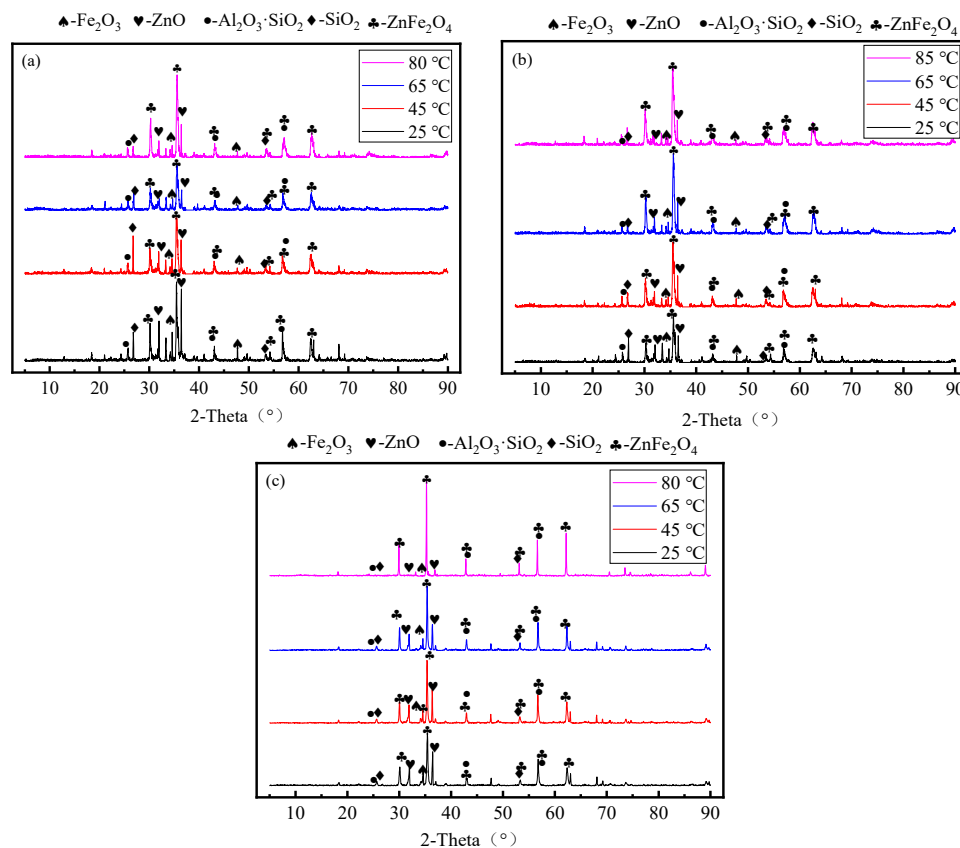


Figure 4. XRD patterns of leaching residue at different leaching temperatures at different sulfuric acid concentrations: (a) 40 g/L; (b) 80 g/L; and (c) 140 g/L.

As shown in Figure 4a, at a low sulfuric acid concentration (40 g/L) and lower leaching temperatures, there are more impurities in leaching residues, and the diffraction peaks of Fe_2O_3 and ZnO are expected. When leaching the temperature increases, the diffraction peak intensities of Fe_2O_3 and ZnO decrease considerably. This indicates that at low sulfuric acid concentrations, leaching temperature has a considerable effect on impurity removal. As shown in Figure 4b, at a moderate sulfuric acid concentration (80 g/L), the diffraction peak intensities of impurities in the XRD spectra of the leaching residues at various leaching temperatures are weaker than those at low sulfuric acid concentrations. Furthermore, as leaching temperature increases, the diffraction peak intensities of Fe_2O_3 and ZnO do not considerably decrease. As seen in Figure 4c, at a high sulfuric acid concentration (140 g/L), the diffraction peaks of Fe_2O_3 and ZnO disappear at low leaching temperatures. However, if the leaching temperature is too high, the diffraction peak intensity of zinc ferrite decreases.

Therefore, at low sulfuric acid concentrations, leaching temperature has a considerable effect on the purification of zinc ferrite; the higher the sulfuric acid concentration, the lower the effect of leaching temperature. This may be attributed to the low concentration of H^+ in the solution when sulfuric acid concentration is low. Increasing the temperature of the solution can effectively increase the diffusion rate of H^+ , thereby enhancing the probability of H^+ reacting with Fe_2O_3 and ZnO and promoting the dissolution reaction. When the sulfuric acid concentration increases, the concentration of H^+ in the solution increases, and the effect of increasing the temperature of the solution to enhance the reaction between H^+ and the reactant is weakened. Therefore, at a sulfuric acid concentration of 80 g/L, increased leaching temperature has a lower effect on the purification of zinc ferrite than at a sulfuric acid concentration of 40 g/L. When the concentration of sulfuric acid reaches 140 g/L, leaching temperature causes the dissolution of zinc ferrite in the sample, which is reflected in the XRD spectrum as a weakened diffraction peak of zinc ferrite. According to

the XRD quantitative analysis, zinc ferrite content in the leaching residues at sulfuric acid concentrations of 140, 80, and 40 g/L at a leaching temperature of 80 °C are 91%, 85.8%, and 85.3%, respectively.

3.3. Effect of Liquid–Solid Ratio

The liquid–solid ratio test conditions are as follows: 50 g of Sample B is used; sulfuric acid concentrations is 40, 80, and 160 g/L; leaching temperature is 80 °C; leaching time is 120 min; stirring speed is 300 rpm; and liquid–solid ratios are 3:1, 4:1, 5:1, 6:1, 7:1, 8:1, 9:1, and 10:1. The effect of liquid–solid ratios on the content of zinc ferrite in the leaching residues is depicted in Figure 5.

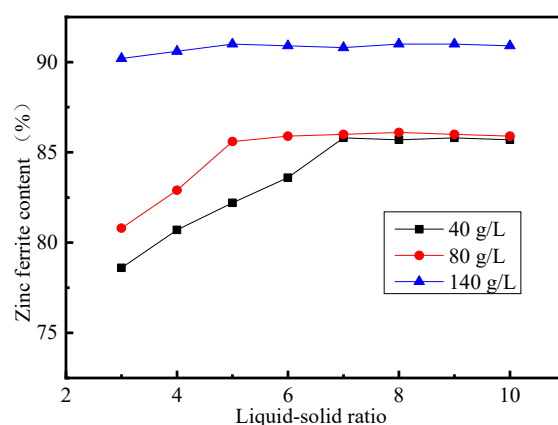


Figure 5. Effect of liquid–solid ratios on zinc ferrite content in leaching residues at different sulfuric acid concentrations.

As shown in Figure 5, at sulfuric acid concentrations of 40 and 80 g/L and as the liquid–solid ratio increases, zinc ferrite content in the leaching residues also increases. At a sulfuric acid concentration of 40 g/L and a liquid–solid ratio of 7:1, zinc ferrite content in the leaching residues reaches 85.3%, and then, the zinc ferrite content tends to stabilize. Similarly, at a sulfuric acid concentration of 80 g/L and a liquid–solid ratio of 5:1, zinc ferrite content in the leaching residues reaches 85.8%, and then, the zinc ferrite content tends to stabilize. As seen in Figure 5, at a sulfuric acid concentration of 140 g/L, the liquid–solid ratio has low effect on zinc ferrite content in the leaching residues. When the liquid–solid ratio is 3:1, zinc ferrite content in the leaching residues reaches 91%. The above difference is due to the fact that at sulfuric acid concentrations of 40 and 80 g/L, only some easily soluble impurity minerals are dissolved. As the liquid–solid ratio increases, the zinc ferrite content no longer increases after the soluble impurity minerals are dissolved. At a high sulfuric acid concentration of 140 g/L, other insoluble impurities in the leaching residues are also dissolved and the zinc ferrite content in the leaching residues reaches 91%. Furthermore, high sulfuric acid concentrations almost completely dissolve impurities when the liquid–solid ratio is 3:1.

The XRD spectra of the leaching residues with different liquid–solid ratios and sulfuric acid concentrations are shown in Figure 6.

Figure 6 shows that the XRD patterns of the leaching residues with different liquid–solid ratios and sulfuric acid concentrations considerably differ. As seen in Figure 6a, at a sulfuric acid concentration of 40 g/L, the diffraction peak intensities of Fe_2O_3 and ZnO in the sample considerably decrease with an increase in the liquid–solid ratio. When the liquid–solid ratio is 7:1, the diffraction peaks of Fe_2O_3 and ZnO disappear. As seen in Figure 6b, at a sulfuric acid concentration of 80 g/L and a liquid–solid ratio of 5:1, the diffraction peaks of impurity minerals disappear. Similarly, as seen in Figure 6c, at a sulfuric acid concentration of 140 g/L and a liquid–solid ratio of 3:1, the impurity peaks in the sample disappear.

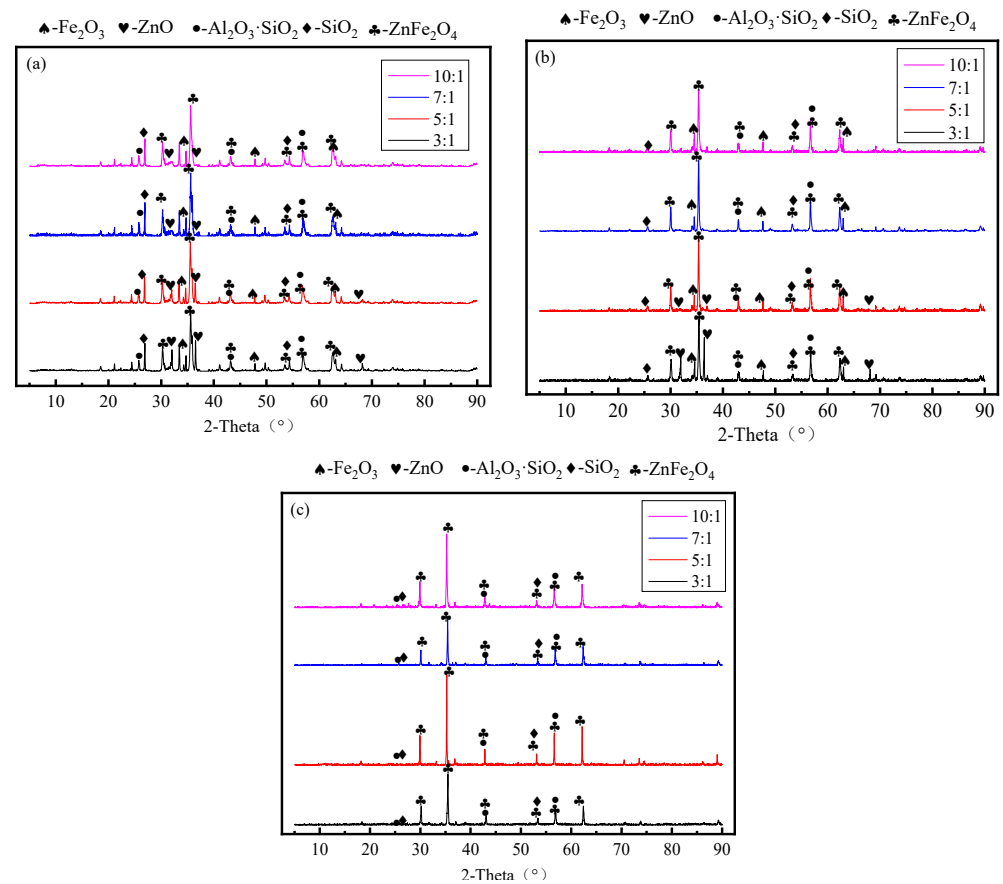


Figure 6. The XRD spectra of the leaching residues with different liquid–solid ratios and sulfuric acid concentrations: (a) 40 g/L; (b) 80 g/L; and (c) 140 g/L.

3.4. Effect of Leaching Time

The leaching time test conditions are as follows: 50 g of Sample B is used, liquid–solid ratio is 7:1; leaching temperature is 80 °C; leaching times are 10, 20, 30, 45, 60, 90, 120, 150, and 200 min; stirring speed is 300 rpm; and sulfuric acid concentrations are 40, 80, and 140 g/L. The effect of leaching time at different sulfuric acid concentrations on the content of zinc ferrite in the leaching residues is depicted in Figure 7.

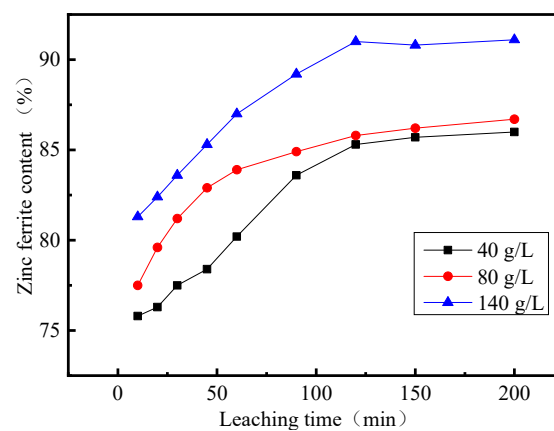


Figure 7. Effect of leaching time on zinc ferrite content in the leaching residues at different sulfuric acid concentrations.

As seen in Figure 7, as leaching time is increased, the content of zinc ferrite in the sample gradually increases. At sulfuric acid concentrations of 40 and 80 g/L, zinc ferrite

content did not change considerably after 120 min of leaching. When the sulfuric acid concentration is 140 g/L, zinc ferrite content was unchanged after 120 min of leaching.

The XRD spectra of zinc ferrite in the sulfuric acid leaching residues with different leaching times and sulfuric acid concentrations of 40, 80, and 140 g/L are shown in Figure 8.

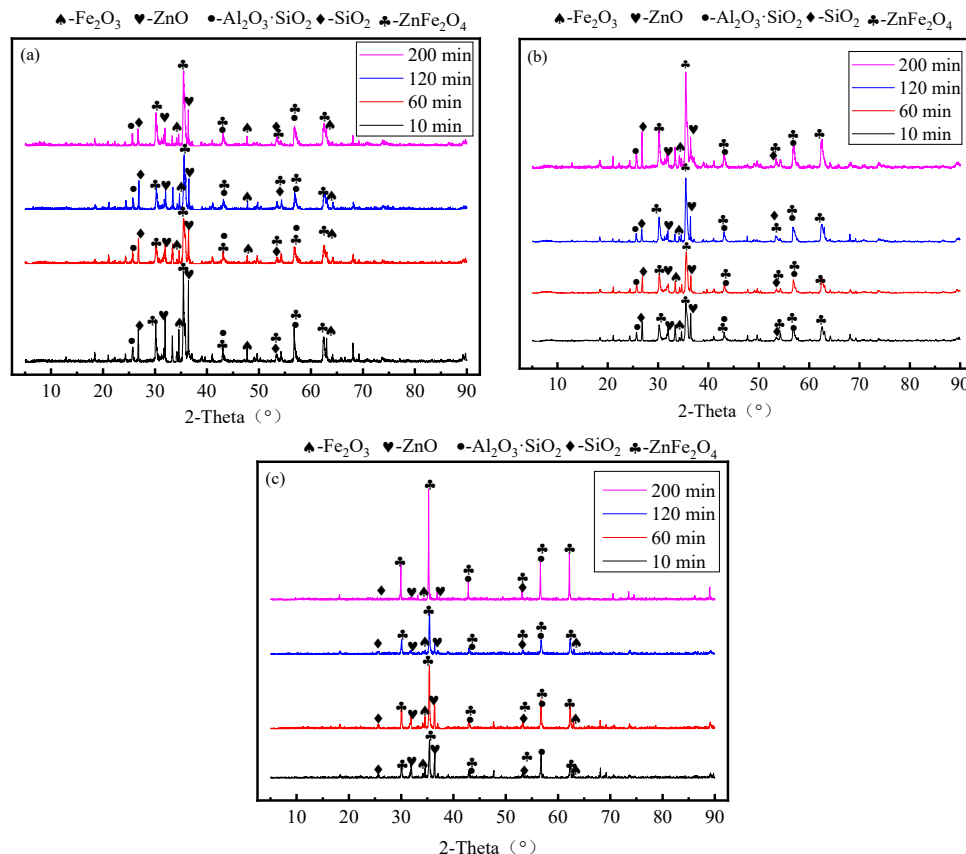


Figure 8. XRD patterns of the leaching residues with different leaching times at different sulfuric acid concentrations: (a) 40 g/L; (b) 80 g/L; and (c) 140 g/L.

As seen in Figure 8a,b, as leaching time is increased, the diffraction peak intensities of Fe_2O_3 and ZnO decrease. When the concentration of sulfuric acid is low (40 and 80 g/L), even after leaching for 200 min, Fe_2O_3 and ZnO exist in the leaching residues. The differences in XRD peaks are considerable for leaching times of 10–120 min, and there are only slight differences in XRD patterns for leaching times exceeding 120 min. As seen in Figure 8c, at a sulfuric acid concentration of 140 g/L, the XRD patterns differ considerably under different leaching times. As the leaching time is increased, the diffraction peak intensities of Fe_2O_3 and ZnO decrease rapidly. When the leaching time reaches 120 min, almost no diffraction peaks of Fe_2O_3 and ZnO are observed. Moreover, the diffraction peak intensities of zinc ferrite are high, indicating that the purity of zinc ferrite in the leaching residues is high: zinc ferrite content reaches 91%.

3.5. Effect of Stirring Speed

The test conditions for different leaching stirring speeds are as follows: 50 g of Sample B is used; liquid–solid ratio is 7:1; leaching temperature is 80 °C; leaching time is 120 min; stirring speeds are 0 (no stirring); 100, 200, 300, 400, 500, and 600 rpm; and sulfuric acid concentrations of 40, 80, and 140 g/L. The effect of stirring speed on the content of zinc ferrite in the leaching residues at different sulfuric acid concentrations is depicted in Figure 9.

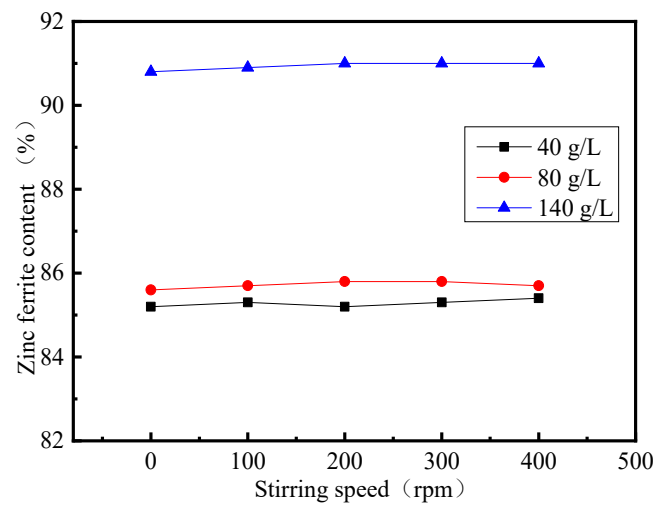


Figure 9. Effect of stirring speed on zinc ferrite content in the leaching residues at different sulfuric acid concentrations.

As seen in Figure 9, the slopes of the three curves are almost constant, indicating that stirring speed has no considerable effect on the purification effect of sulfuric acid leaching.

At the sulfuric acid concentration of 140 g/L, the liquid–solid ratio is 4:1; the leaching temperature is 80 °C; stirring speeds are 0, 100, 200, 300, and 400 rpm; and leaching times are 10, 20, 30, 60, 90, 120, 150, 200, 250, and 300 min. The effect of leaching time on the content of zinc ferrite in the leaching residues at different stirring speeds is depicted in Figure 10.

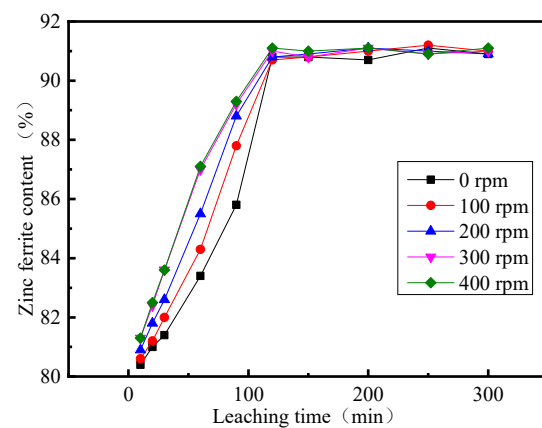


Figure 10. Effect of leaching time on zinc ferrite content in the leaching residues at different stirring speeds.

As seen in Figure 10, stirring speed is only related to the dissolution rate of the leaching residues and not to the final dissolution result. Increasing stirring speed accelerates the dissolution rate of the sample in the solution, which is reflected in the different slopes of the stirring speed curves: the higher the stirring speed, the higher the slope of the curve. Note that curves corresponding to the stirring speeds of 300 and 400 rpm almost coincide, indicating that when the stirring speed is >300 rpm, increasing stirring speed has a low effect on the purification effect of leaching.

At the sulfuric acid concentration of 140 g/L, the liquid–solid ratio is 4:1; the leaching temperature is 80 °C; leaching times are 10, 60, and 120 min; and stirring speeds are 0, 100, 200, 300, and 400 rpm. The XRD spectra of the leaching residues under different leaching times and stirring speeds are shown in Figure 11.

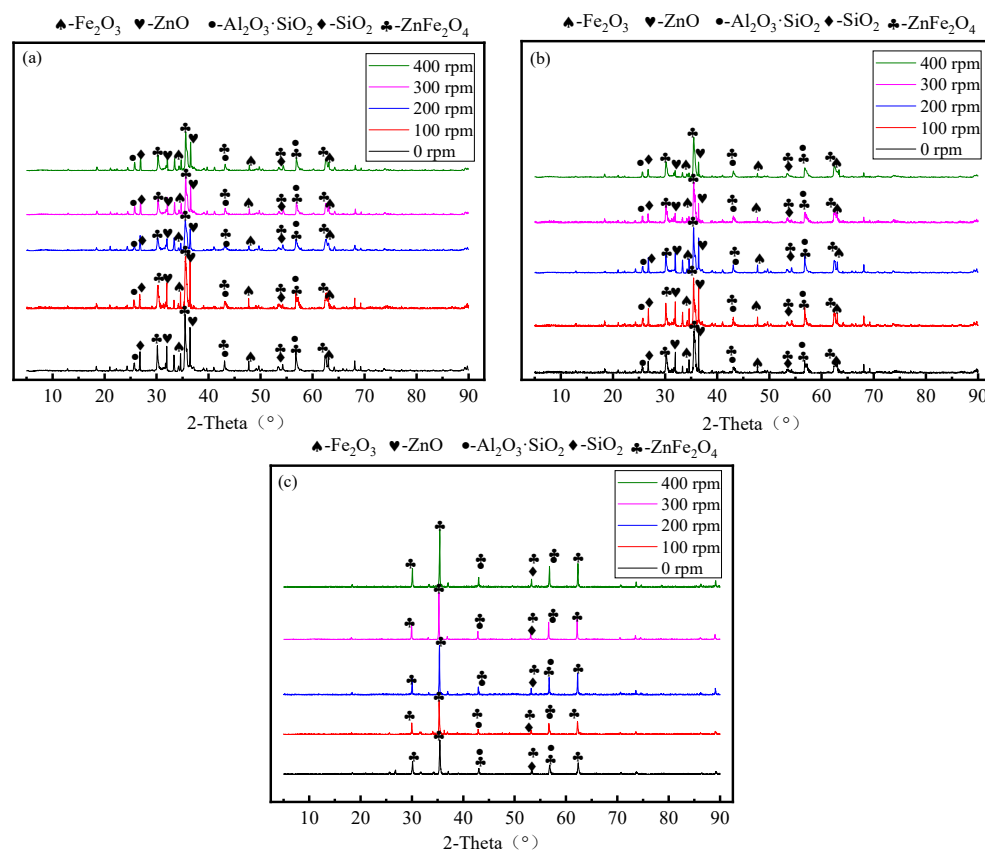


Figure 11. XRD spectra of the leaching residues under different stirring speeds and leaching times: (a) 10 min; (b) 60 min; and (c) 120 min.

As seen in Figure 11, under different leaching times, the content of each component in the leaching residues obtained under different stirring speeds differs. For a leaching time of 10 min, the diffraction peak intensities of Fe_2O_3 and ZnO in the residues are high at the stirring speed set in the experiment. For a leaching time of 60 min, as stirring speed is increased, the diffraction peak intensities of Fe_2O_3 and ZnO decrease while that of zinc ferrite increase. This indicates that increasing the stirring speed has a considerable effect on the dissolution rate increment. When the leaching time is 120 min, the XRD peaks of the samples are similar under different stirring speeds, and the diffraction peaks of Fe_2O_3 and ZnO almost disappear. Under this leaching time, most soluble impurities are dissolved.

4. Conclusions

(1) For Sample A, the purification effect of sulfuric acid leaching is insignificant, and zinc ferrite content in the residues only increases by 2.1%. For Sample B, the purification effect of sulfuric acid leaching is as expected and zinc ferrite content in the residues increases by 15.7%. When leaching time is optimal, sulfuric acid concentration has a considerable effect on zinc ferrite content in the leaching residues. When sulfuric acid concentration is 140 g/L, Fe_2O_3 and ZnO in the sample are completely dissolved; however, the dissolution of zinc ferrite is gradual, which is beneficial to the purification of zinc ferrite.

(2) The higher the sulfuric acid concentration, the lower the effect of leaching temperature. When the liquid–solid ratio is 7:1, the leaching temperature is 80 °C, and the leaching time is 120 min, the following is observed: when sulfuric acid concentration is 140 g/L, 80g/L, and 40 g/L, zinc ferrite content in the leaching residues reaches 91%, 85.8%, and 85.3%, respectively.

(3) As the leaching time is increased, the reaction in the solution proceeds gradually, and for a leaching time of 120 min, the sample dissolution curve tends to stabilize. Stirring speed only affects the rate at which the sample is dissolved and not the degree to which

the solution dissolves the sample. Increasing stirring speed benefits the dissolution rate of impurities in the sample. When the stirring speed is 300 rpm, the promoting effect of stirring speed on the dissolution rate reaches its limit.

(4) The conditions suitable for preparing zinc ferrite products by sulfuric acid leaching, purification, and roasting are as follows: The sulfuric acid concentration is 140 g/L, the liquid–solid ratio is 4:1, the leaching temperature is 80 °C, the leaching time is 120 min, and the stirring speed is 300 rpm. Under these conditions, the content of zinc ferrite in the leaching residue is about 91%.

Author Contributions: Conceptualization, J.Y. and H.L. (Hengjun Li); data curation, Z.L. and H.L. (Hangyu Li) formal analysis, X.H. and S.L.; funding acquisition, J.Y.; investigation, S.L.; methodology, J.Y. and S.M.; project administration, J.Y. and H.L. (Hengjun Li); validation, H.L. (Hangyu Li) and Z.L.; writing—original draft, H.L. (Hengjun Li) and J.Y.; writing—review and editing, J.Y. and S.M. All authors have read and agreed to the published version of the manuscript.

Funding: This research was funded by the National Natural Science Foundation of China (No. 52264020, No. 51774099).

Data Availability Statement: Not applicable.

Conflicts of Interest: The authors declare no conflict of interest.

References

- Ma, S.; Li, H.; Yang, X.; Xu, W.; Deng, X.; Yang, J. Study on Impact Crushing Characteristics of Minerals Based on Drop Weight Tests. *Minerals* **2023**, *13*, 632. [[CrossRef](#)]
- Hayes, S.M.; Root, R.A.; Perdrial, N.; Maier, R.M.; Chorover, J. Surficial weathering of iron sulfide mine tailings under semi-arid climate. *Geochim. Cosmochim. Acta* **2014**, *141*, 240–257. [[CrossRef](#)]
- Kříbek, B.; Zachariáš, J.; Knésl, I.; Míková, J.; Mihaljevič, M.; Veselovský, F.; Bamba, O. Geochemistry, mineralogy, and isotope composition of Pb, Zn, and Cu in primary ores, gossan and barren ferruginous crust from the Perkoa base metal deposit, Burkina Faso. *J. Geochem. Explor.* **2016**, *168*, 49–64. [[CrossRef](#)]
- Baggio, S.B.; Hartmann, L.A.; Massonne, H.J.; Theye, T.; Antunes, L.M. Silica gossan as a prospective guide for amethyst geode deposits in the Ametista do Sul mining district, Paraná volcanic province, southern Brazil. *J. Geochem. Explor.* **2015**, *159*, 213–226. [[CrossRef](#)]
- Yesares, L.; Sáez, R.; Ruiz De Almodóvar, G.; Nieto, J.M.; Gómez, C.; Ovejero, G. Mineralogical evolution of the Las Cruces gossan cap (Iberian Pyrite Belt): From subaerial to underground conditions. *Ore Geol. Rev.* **2017**, *80*, 377–405. [[CrossRef](#)]
- Laakso, K.; Rivard, B.; Rogge, D. Enhanced detection of gossans using hyperspectral data: Example from the Cape Smith Belt of northern Quebec, Canada. *ISPRS J. Photogramm. Remote Sens.* **2016**, *114*, 137–150. [[CrossRef](#)]
- Velasco, F.; Herrero, J.M.; Suárez, S.; Yusta, I.; Alvaro, A.; Tornos, F. Supergene features and evolution of gossans capping massive sulphide deposits in the Iberian Pyrite Belt. *Ore Geol. Rev.* **2013**, *53*, 181–203. [[CrossRef](#)]
- Costa, M.L.; Angélica, R.S.; Costa, N.C. The geochemical association Au-As-B-(Cu)-Sn-W in latosol, colluvium, lateritic iron crust and gossan in Carajás, Brazil: Importance for primary ore identification. *J. Geochem. Explor.* **1999**, *67*, 33–49. [[CrossRef](#)]
- Assawincharoenkij, T.; Hauenberger, C.; Ettinger, K.; Sutthirath, C. Mineralogical and geochemical characterization of waste rocks from a gold mine in northeastern Thailand: Application for environmental impact protection. *Environ. Sci. Pollut. Res. Int.* **2018**, *25*, 3488–3500. [[CrossRef](#)]
- Lorenzo-Tallafigo, J.; Iglesias-González, N.; Mazuelos, A.; Romero, R.; Carranza, F. An alternative approach to recover lead, silver and gold from black gossan (polymetallic ore). Study of biological oxidation and lead recovery stages. *J. Clean. Prod.* **2019**, *207*, 510–521. [[CrossRef](#)]
- Mohamed, M.; Saleh, Q.; Mohamed, S.A.; Yasser, F.S.; Ahmed, M.A. Insights into the adsorption performance and mechanism of Cr(VI) onto porous nanocomposite prepared from gossans and modified coal interface: Steric, energetic, and thermodynamic parameters interpretations. *Chin. J. Chem. Eng.* **2023**, *in press*. [[CrossRef](#)]
- Dunn, S.C.; von der Heyden, B.P. Gold remobilization in gossans of the Amani area, southwestern Tanzania. *Ore Geol. Rev.* **2021**, *131*, 104033. [[CrossRef](#)]
- Santoro, L.; Putzolu, F.; Mondillo, N.; Boni, M.; Herrington, R. Influence of genetic processes on geochemistry of Fe-oxy-hydroxides in supergene Zn non-sulfide deposits. *Minerals* **2020**, *10*, 602. [[CrossRef](#)]
- Yang, J.L. Research on the Separation and Recovery of Zinc and Iron from Gossan Ores. Ph.D. Thesis, Guangxi University, Nanning, China, 2012. (In Chinese)
- Yang, J.; Li, Z.; Huo, X.; Li, H.; Liao, S.; Ma, S.; Li, H. Study on the Preparation of ZnFeO₄ by Roasting Zinc-Containing Gossan Ore. *Processes* **2023**, *11*, 1991. [[CrossRef](#)]
- Pannaparayil, T.; Komarneni, S.; Marande, R.; Zadarko, M. Subdomain zinc ferrite particles: Synthesis and characterization. *J. Appl. Phys.* **1990**, *67*, 5509–5511. [[CrossRef](#)]

17. Kazantseva, N.E.; Bespyatykh, Y.I.; Sapurina, I.; Stejskal, J.; Vilčáková, J.; Sába, P. Magnetic materials based on manganese-zinc ferrite with surface-organized polyaniline coating. *J. Magn. Magn. Mater.* **2006**, *301*, 155–165. [[CrossRef](#)]
18. Yang, J.; Xu, S.; Zhu, P. Comparative study on properties of zinc ferrite and its purified products. *J. Phys. Conf. Ser.* **2021**, *2044*, 012068. [[CrossRef](#)]
19. Ismail, M.; Hao, A.; He, S.; Huang, W.; Qin, N.; Bao, D. Reversible transitions among four modes of nonpolar resistive switching characteristics in nano-crystalline zinc ferrite magnetic thin films. *J. Alloys Compd.* **2018**, *753*, 100–110. [[CrossRef](#)]
20. Ehrhardt, H.; Campbell, S.J.; Hofmann, M. Magnetism of the nanostructured spinel zinc ferrite. *Scr. Mater.* **2003**, *48*, 1141–1146. [[CrossRef](#)]
21. Hankare, P.P.; Patil, R.P.; Jadhav, A.V.; Garadkar, K.M.; Sasikala, R. Enhanced photocatalytic degradation of methyl red and thymol blue using titania-alumina-zinc ferrite nanocomposite. *Appl. Catal. B* **2011**, *107*, 333–339. [[CrossRef](#)]
22. Jadhav, S.V.; Jinka, K.M.; Bajaj, H.C. Nanosized sulfated zinc ferrite as catalyst for the synthesis of nopol and other fine chemicals. *Catal. Today* **2012**, *198*, 98–105. [[CrossRef](#)]
23. Li, Q.; Zhuang, L.; Chen, S.; Xu, J.; Li, H. Preparation of carbon-supported zinc ferrite and its performance in the catalytic degradation of mercaptan. *Energy Fuels* **2012**, *26*, 7092–7098. [[CrossRef](#)]
24. Yang, J.; Zhu, P.; Ma, S. Study on properties of gossan ore from zinc sulfide deposit. *J. Phys. Conf. Ser.* **2021**, *2044*, 012081. [[CrossRef](#)]

Disclaimer/Publisher's Note: The statements, opinions and data contained in all publications are solely those of the individual author(s) and contributor(s) and not of MDPI and/or the editor(s). MDPI and/or the editor(s) disclaim responsibility for any injury to people or property resulting from any ideas, methods, instructions or products referred to in the content.